

# Thermal analysis of hexadecyltrimethylammonium-montmorillonites

## Part 2. Thermo-XRD-spectroscopy-analysis

Isaak Lapidés · Mikhail Borisover ·  
Shmuel Yariv

Niinistö's Special Chapter  
© Akadémiai Kiadó, Budapest, Hungary 2011

**Abstract** Na-montmorillonite (Na-MONT) was loaded with hexadecyltrimethylammonium cations (HDTMA) by replacing 41 and 90% of the exchangeable Na with HDTMA. The organoclays were labeled OC-41 and OC-90, respectively. Freeze-dried Na-MONT, OC-41, and OC-90 were heated in air at 150, 250, 360, 420, 550, 700, and 900 °C. The thermally treated samples were suspended in water, air-dried, and desiccated over silica during 40 days. All samples were diffracted by X-ray and fitting calculations were performed on each diffractogram. These calculations gave information on basal spacings, relative concentrations, and homogeneity of the different tactoids obtained at each temperature, before and after suspending and desiccating. HDTMA-MONT tactoids with spacing  $\geq 1.41$  nm appeared between 25 and 250 °C. OC-41 or OC-90 intercalated monolayers or bilayers of HDTMA, respectively. At 250 °C OC-41 was air-oxidized to a smaller extent than OC-90, resulting in charcoal-MONT tactoids. With further heating the organic matter was gradually oxidized and at 700 °C both clays were collapsed. During the thermo-XRD-analysis of both organoclays three types of charcoal-MONT complexes appeared: (1) LTSC-MONT tactoids with a basal spacing 1.32–1.39 nm, between 250 and 420 °C in both clays; (2)

HTSC- $\alpha$ -MONT tactoids with spacing 1.22–1.28 nm, between 360 or 250 and 500 or 550 °C in OC-41 or OC-90, respectively; (3) HTSC- $\beta$ -MONT with spacing 1.12–1.18 nm, between 360 and 550 °C in both clays, where LTSC and HTSC are low- and high-temperature stable charcoal, respectively. HTSC- $\beta$ -MONT differs from HTSC- $\alpha$ -MONT by having carbon atoms keying into the ditrigonal holes of the clay-O-planes.

**Keywords** Hexadecyltrimethylammonium ·  
Montmorillonite · Organoclays · Tactoids ·  
Thermal analysis · X-ray

## Introduction

Clay minerals, in which the natural exchangeable inorganic cations have been replaced by organic cations, are termed organoclays [1, 2]. In their natural state smectite clays are hydrophilic, due to the presence of metallic cations in the interlayers. Loading them with cationic surfactants converts the hydrophilic galleries into organophilic [3]. Organoclays obtained by modifying Na- or Ca-smectites with alkylammonium cations, mainly with quaternary ammonium cations, are used as sorbents of different organic molecules from aqueous systems [4]. In recent years our research has been focused on the adsorption abilities of non-charged organic molecules by the organoclay obtained by modifying montmorillonite (MONT) with different loadings with the cationic surfactant hexadecyltrimethylammonium (HDTMA) and on the effect of preheating the organoclay on its adsorption abilities [5]. For this purpose two types of the organoclays (OC) were used. They were prepared by loading MONT with 41 and 90 percent of its cation exchange

I. Lapidés · S. Yariv (✉)  
Institute of Chemistry, The Hebrew University of Jerusalem,  
Campus Edmund Y. Safra, 91904 Jerusalem, Israel  
e-mail: yarivs@vms.huji.ac.il

M. Borisover  
Institute of Soil, Water and Environmental Sciences,  
The Volcani Center, Agricultural Research Organization,  
POB 6, 50250 Bet Dagan, Israel

capacity (CEC) with HDTMA and were labeled OC-41 and OC-90, respectively [6, 7]. The unloaded Na-MONT and each organoclay sample were heated 2 h in ambient atmosphere at 150, 250, 360, and 420 °C and used as sorbents [5].

When organoclays are heated in air, the organic cations are thermally oxidized in several steps [8–13]. In the first step of the thermal oxidation of the organic cation most of the organic hydrogen is oxidized into water, but only part of the carbon and nitrogen are oxidized into CO<sub>2</sub> and NO<sub>2</sub>, respectively, evolving from the system [8–11, 14]. The non-evolved carbon and nitrogen form two types of intercalated charcoal. One type is oxidized at a lower temperature than the other (second and third steps of oxidation, respectively). They are named low- and high-temperature stable charcoal, labeled LTSC and HTSC, respectively [8]. The thermal oxidation of the organic cation is accompanied by mass loss and the different steps are presented in a DTA curve by exothermic peaks. Another type of mass loss results from the dehydration and dehydroxylation of the clay. The latter reactions are presented in a DTA curve by two endothermic peaks [15].

Very little is known about the structure and properties of the different charcoal-clay tactoids. More information is required in order that these nanocomposite materials will be applied in modern technologies [16].

The purpose of the present study is to investigate the composition and properties of the thermally treated OC-41 and OC-90. In addition to the above mentioned temperatures of the thermal treatment, samples were heated at 550, 700, and 900 °C. In the first part of this study [17] we described TG curves of Na-MONT, OC-41, and OC-90. Carbon and hydrogen contents in each of the unheated and heated samples were determined and their IR spectra were recorded. It was shown that at room temperature and at 150 °C HDTMA cations persisted in the interlayers of OC-41 and OC-90. At 250 °C in OC-41 some HDTMA cations were oxidized to volatile H<sub>2</sub>O and nonvolatile intercalated charcoal, whereas in OC-90 most HDTMA was oxidized into volatile H<sub>2</sub>O and nonvolatile intercalated charcoal. After heating at 360 °C charcoal was present in both organoclays. Charcoal persisted at 420 °C in both clays but was gradually oxidized to CO<sub>2</sub> at higher temperatures. These results are in agreement with our interpretation of the DTA curves of HDTMA-MONT, which were recorded by He et al. [18].

Thermo-XRD-analysis of organoclays was previously described [19]. This study deals with thermo-XRD-analysis of freeze-dried Na-MONT, OC-41, and OC-90. The unheated and heated samples are diffracted by X-ray, and fitting calculations are performed on each diffractogram. These calculations give information on the tactoids obtained at each temperature, basal spacings, relative concentrations, and homogeneity.

The freeze-dried and thermally treated samples are suspended in water and basal spacings are determined by XRD. Fitting calculations on the diffractograms give information on swelling of the different tactoids obtained during heating.

After suspending, the samples are desiccated in the presence of silica during 40 days and diffracted by X-ray. Curve fitting calculations on these diffractograms supply information on the dehydration and collapse abilities of the different tactoids which are present in the samples. This information is essential to our understanding of the swelling and contraction abilities of the thermally treated organoclays during the adsorption study of non-charged organic compounds from aqueous solutions.

## Experimental

Materials used in this study (Na-MONT and HDTMABr), and the preparation methods of OC-41 and OC-90, were previously described [6, 7].

In the present thermo-XRD analysis study three different series of diffractions were recorded for Na-MONT, OC-41, and OC-90. In the first series the effect of the thermal treatment on the basal spacings of the three clays was determined. For this purpose few milligrams of Na-MONT and of the two organoclays were heated during 2 h at 150, 250, 360, 420, 550, 700, and 900 °C in air atmosphere. Mass loss due to the evolution of surface and interlayer water, thermal dehydroxylation of the clay, and air-oxidation of the organic matter were calculated from the TG curves of the samples shown in part 1 of this study [17]. Powders of freeze-dried unheated and thermally treated samples were diffracted by X-ray.

In the second series the effect of suspending in water on the basal spacings of the unheated and thermally treated clays was determined. For this purpose few grains of a sample was suspended in five drops of water. After being thoroughly shaken for 10 min the suspensions were poured on glass slides, air-dried overnight, and the oriented samples were diffracted by X-ray. Diffractograms of this series supply information on the effect of thermal treatments on swelling abilities of the samples.

In the third series the effect of desiccating under silica on the basal spacings of the suspended unheated and thermally treated Na-MONT, OC-41, and OC-90 was determined. For this purpose glass slides with the air-dried suspended samples were left in a desiccator containing silica. After 40 days the slides with the desiccated clays were diffracted by X-ray. Preliminary experiments showed that 40 days were necessary to achieve reproducible results. This series gives information on the effect of the thermal treatments on the contraction and collapse abilities of the samples.

X-ray diffractograms of powder (first series) or oriented samples (second and third series) were recorded at room temperature, under ambient atmosphere, using a Philips Automatic Diffractometer (PW 1710) with a Cu tube anode. Diffractograms recorded during the thermo-XRD-analysis were fitted by 'PHILIPS' Automatic Powder Diffraction (PW1877/43) software, version 3.5. Profile Fitting is used for accurate determination of peak positions, widths, backgrounds, and intensities (relative peak component areas). This method is useful especially when lines of interest in the diffractogram are obscured by overlapping peaks, or when a complex background is present. Gaussian shapes were used for the peaks. The fitting method was previously described [13].

## Results and discussion

Thermal amorphization of MONT occurs simultaneously with dehydroxylation [15]. Intensities of its characteristic X-ray peaks are slightly decreased after heating the clays at 420 °C, and further decrease after 550 and 700 °C, relative to the intensity of the characteristic quartz peak at 0.335 nm, which is present as impurity in the Wyoming bentonite. Diffractograms of samples heated at 900 °C do not show peaks of MONT. They are described after those of samples gradually heated up to 700 °C.

The curve fitting calculations on the different X-ray diffractograms result in a single-, two-, or three-peak components. Each of these peak components characterizes one type of tactoids (clusters composed of several parallel face-to-face TOT layers). Location of its maximum (in nm) describes the basal spacing of the respective tactoid. Relative peak component area (in percent from the total peak area) shows the relative concentration of the respective tactoid in the stack. The width of the peak component (in  $^{\circ}2\theta$ ) represents the homogeneity of the respective tactoid. A homogeneous stack of tactoids poses a small component width whereas an inhomogeneous stack poses a broad width. In this article, if a single peak component results from the curve fitting calculations, it is labeled by X. If two or three components are obtained, they are labeled by A, B, and C. Tactoids (or peak components) with the largest spacing are labeled by A, those with a smaller spacing by B and those with the smallest by C. No fitting results with more than three components are obtained in this study.

Two types of charcoal were identified from DTA and TG curves, low- and high-temperature stable charcoal (LTSC and HTSC, respectively) [10–12]. In this study we are going to show that XRD identifies two types of tactoids with high-temperature stable charcoal. They are labeled by  $\alpha$  and  $\beta$  as follows, HTSC- $\alpha$  and HTSC- $\beta$ , respectively.

## Na-montmorillonite

### First series

The results of curve fitting calculations of X-ray-diffractograms recorded during the thermo-XRD-analysis (maxima of peak components in nm, their relative areas in % of the total peak area and width at half heights in  $^{\circ}2\theta$ ) of freeze-dried Na-MONT, before and after thermal treatments, are plotted in Fig. 1. The fitted diffractogram of unheated sample shows a single peak with a maximum at 1.17 nm, characteristic for tactoids with intercalated compacted water monolayers [20]. The peak is broad with a width at half height of 2.83  $^{\circ}2\theta$ , indicating that the tactoid stack is inhomogeneous.

According to the TG curve previously described [17], at 150 °C Na-MONT loses 8.6% due to the evolution of surface and interlayer water. The curve fitted diffractogram of this sample shows a single peak component with a maximum at 1.26 nm and a width at half height of 2.83  $^{\circ}2\theta$ , indicating the presence of inhomogeneous stack of tactoids with intercalated water monolayers [20]. The basal spacing of the unheated sample is smaller than that of the thermally treated sample, indicating that the latter has been rehydrated by adsorbing water from the atmosphere.

Mass loss of 9.1% at 250 °C is due to interlayer water evolution [17]. The fitted diffractogram of Na-MONT heated at 250 °C shows two peak components, A and B, with maxima at 1.10 and 0.98 nm and widths at half heights of 1.57 and 0.65  $^{\circ}2\theta$ , representing an inhomogeneous stack of tactoids with partial dehydration and an homogeneous stack of dehydrated collapsed tactoids, respectively. If we

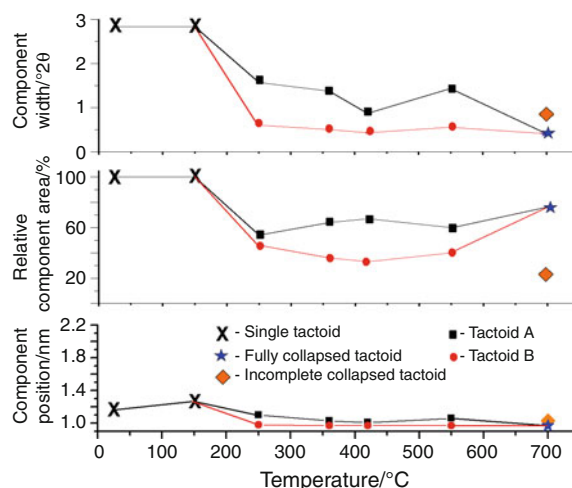


**Fig. 1** Summary of curve fitting calculations on diffractograms of thermo-XRD-analysis of freeze-dried Na-MONT, (first series). *Bottom* maxima of peak components (in nm); *middle* relative component areas (in % of the total peak area); *top* component widths at half heights (in  $^{\circ}2\theta$ )

assume similar diffraction indices for both tactoids, from the relative peak component areas it appears that type A with the larger spacing forms 54% of the stack, whereas type B with the smaller spacing forms 46%. Spacing of 0.98 nm characterizes fully collapsed tactoids [19]. Spacing of 1.10 nm is too short for tactoids with intercalated water monolayers and too large for collapsed tactoids. However, it may occur from regular interstratification of one water layer and anhydrous interlayer [21, 22].

Mass loss between 250 and 360 °C and between 360 and 420 °C of 0.4 and 0.3%, respectively, are due to the last stages of interlayer water evolution [17]. Mass loss in the temperature ranges 420–550, 550–700 and 700–900 °C of 1.2, 3.0 and 1.8%, respectively, are due to the dehydroxylation of the clay [8]. Peak components A ( $70 \pm 3\%$ ) and B ( $30 \pm 3\%$ ) in fitted diffractograms of samples heated at 360–550 °C are at  $1.02 \pm 0.01$  and 0.97 nm, respectively. Both spacings characterize collapsed clay. The larger spacing suggests the presence of tactoids in which keying of the exchangeable cations through the ditrigonal holes of the oxygen planes toward the tetrahedral sheets is incomplete. For keying to occur the exchangeable inorganic cations should be bare. Wyoming MONT contains small amounts of  $\text{Ca}^{2+}$  in the interlayers [23]. During the thermal treatment  $\text{Ca}^{2+}$  may hydrolyze and form  $[\text{Ca}(\text{OH})]^+$  cations [20, 24]. Due to size effect, keying of hydroxy cations is only partial and an incomplete collapse occurs. These tactoids are termed here incomplete collapsed tactoids.

The fitted diffractogram of Na-MONT heated at 700 °C shows two components, at 1.01 and 0.97 nm, indicating the presence of two types of tactoids, the incomplete and the fully collapsed tactoids. At lower temperatures the former is the principal tactoid but at 700 °C it makes only 22% of the stack. Figure 1 shows that the width at half height of component A is broader than that of B, suggesting that in the stack the incomplete collapsed tactoids are less homogeneous than the fully collapsed.

Dehydroxylation of MONT results in an amorphous phase (meta-MONT) which does not diffract X-ray. From 420 °C there is no effect of thermal treatment on the shape of the diffractograms, but the absolute intensities of the MONT peaks decrease relative to that of quartz, which is present as an impurity in the Wyoming bentonite.

## Second series

Unheated and thermal-treated Na-MONT samples are diffracted by X-ray after being suspended in water and overnight air-dried. The clays are oriented in contrast to the non-oriented powders of the first series and the diffractograms show a better resolution. Swelling of a sample indicates its rehydration. Results of curve fitting calculations on the diffractograms of the suspended samples are

depicted in Fig. 2. Comparing Fig. 1 with Fig. 2 reveals that besides Na-MONT heated at 700 °C, the samples swell in the aqueous suspensions.

Fitting calculations on the diffractogram of the suspended freeze-dried Na-MONT result in two peak components with maxima at 1.49 nm and 1.27 nm, characterizing tactoids with intercalated bi- and monolayers water labeled A and B, respectively [20]. From the relative peak component areas it appears that tactoids with water bilayers form 75% and those with monolayers form 25% of the mixture. These results indicate that Na-MONT does not lose its swelling ability in water as a result of freeze-drying. The width at half heights of A and B components are 1.09 and 0.69  $2\theta$ , respectively, suggesting that tactoids intercalated by water bilayers are less homogeneous than those intercalated by monolayers. Comparing these widths with that of the freeze-dried Na-MONT (2.83  $2\theta$ ) indicates that sedimentation Na-MONT from an aqueous suspension results in oriented tactoids with improved homogeneity.

Similar results are obtained for curve fitted diffractograms of air-dried suspended samples which were heated at 150–550 °C, before being suspended in water (preheated samples). Two types of tactoids A and B with spacings of  $1.45 \pm 0.02$  and 1.25 nm are obtained with intercalated bi- and monolayers of water, respectively [20]. These spacings are slightly smaller than those found for the freeze-dried sample indicating that Na-MONT does not lose its swelling ability in water by thermal treatments up to 550 °C. In this temperature range type B tactoids constitute between 16 and 37% of the clay. However, their homogeneity is better than that of type A as can be seen from width at half heights of their peak components (Fig. 2).

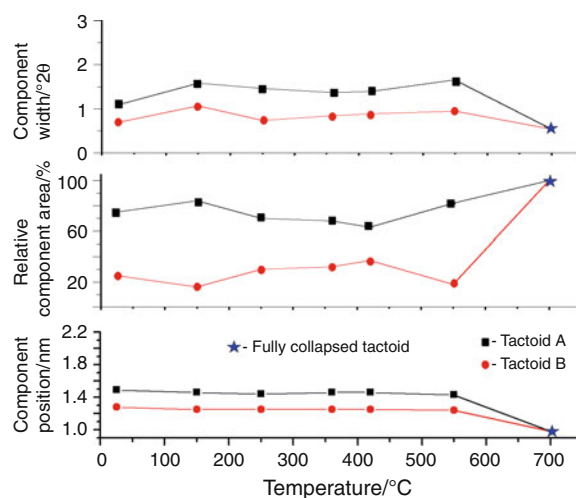


**Fig. 2** Summary of curve fitting calculations on diffractograms of thermo-XRD-analysis of aqueous suspended Na-MONT, (second series). *Bottom* maxima of peak components (in nm); *middle* relative component areas (in % of the total peak area); *top* component widths at half heights (in  $2\theta$ )

Na-MONT heated at 700 °C is fully collapsed and loses its swelling ability in water. From width at half height of peak components it is concluded that tactoids of the collapsed Na-MONT are the most homogeneous among the suspended samples. The incomplete collapsed tactoids which are found before suspending the sample are not present in the suspended sample, probably due to washing out of  $[\text{CaOH}]^+$  cations.

### Third series

Suspended (rehydrated) unheated and preheated Na-MONT samples were left in a desiccator over silica for 40 days. The results of curve fitting calculations made on X-ray diffractograms of these oriented samples are depicted in Fig. 3. Comparing Figs. 1 and 2 with Fig. 3 reveals that besides the sample heated at 700 °C, which does not swell, the rehydrated samples lose only part of the readsorbed water.

Curve fitting calculations on the diffractogram of desiccated unheated Na-MONT shows the presence of two peak components A and B at 1.38 and 1.14 nm with relative peak areas 31 and 69%. Spacing of component A is characteristic for tactoids with incomplete intercalated bilayers of water [13]. It may occur from regular interstratification of tactoids with bi- and mono water layers in the interlayer [21, 22]. Spacing of component B may occur from regular interstratification of tactoids with water monolayer and collapsed interlayer, the latter results from dehydration. Width of peak components indicates that the homogeneity of B is higher than that of A.

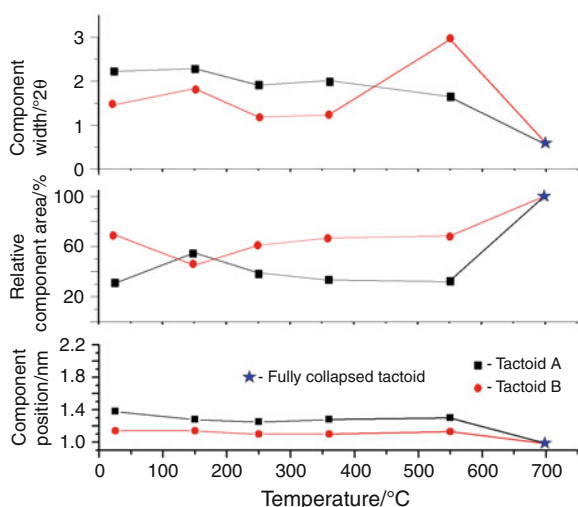


**Fig. 3** Summary of curve fitting calculations on diffractograms of thermo-XRD-analysis of desiccated Na-MONT, (third series). *Bottom* maxima of peak components (in nm); *middle* relative component areas (in % of the total peak area); *top* component widths at half heights (in  $^{\circ}2\theta$ )

Desiccating under silica the suspended Na-MONT preheated at 150–550 °C results in two tactoids with spacings  $1.28 \pm 0.02$  and  $1.12 \pm 0.02$  nm, with relative concentrations 30–40 and 60–70%, labeled A and B, respectively.

As mentioned above, Na-MONT heated at 700 °C does not rehydrate in aqueous suspensions and consequently desiccation has no effect on its basal spacing.

To conclude, the present results show that besides the sample heated at 700 °C, thermally treated Na-MONT does not lose its swelling ability. Desiccated suspended Na-MONT over silica is not completely dehydrated, even after forty desiccation days.

### OC-41

#### First series

Results of curve fitting calculations on diffractograms recorded during thermo-XRD-analysis of powdered freeze-dried OC-41, are depicted in Fig. 4. Calculations on the diffractogram of unheated OC-41 result in two peak components with maxima at 1.50 and 1.41 nm, indicating the presence of two types of tactoids labeled A and B, respectively. Assuming similar diffraction indices to both tactoids, from relative peak component areas it appears that tactoids of type A, with the larger spacing, comprise 42% of the stack whereas those of type B comprise 58%. Both spacings allow the presence of intercalated lateral monolayers of HDTMA. In B the long  $\text{C}_{16}\text{H}_{33}$  chain is lying parallel to the clay-O-plane, whereas in A it is slightly

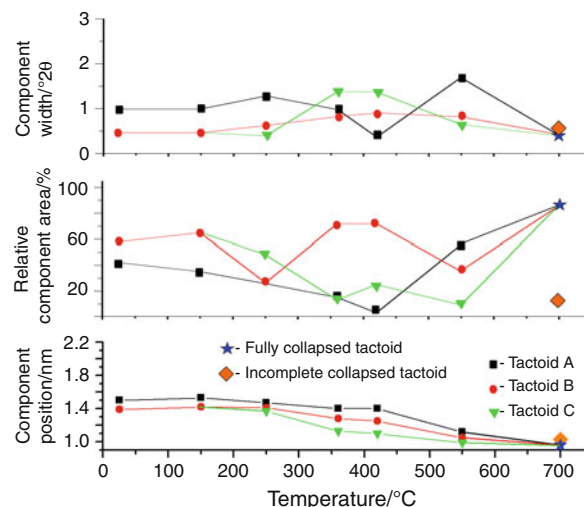


**Fig. 4** Summary of curve fitting calculations on diffractograms of thermo-XRD-analysis of freeze-dried OC-41, (first series). *Bottom* maxima of peak components (in nm); *middle* relative component areas (in % of the total peak area); *top* component widths at half heights (in  $^{\circ}2\theta$ )

tilted. The peak components, with width at half heights of 0.99 and 0.47  $^{\circ}2\theta$ , respectively, are smaller than that in the diffractogram of Na-MONT (2.83  $^{\circ}2\theta$ ) indicating that tactoids of both types of OC-41 are more homogeneous than those of Na-MONT.

According to the TG curve published in the first part of this study, at 150  $^{\circ}\text{C}$  mass loss of OC-41 is 4.4% [17]. There is no carbon loss at this temperature and it is concluded that only water is evolved at this temperature and no organic matter. The fitted X-ray diffractogram of this sample shows two peak components with maxima at 1.53 and 1.41 nm, indicating the presence of two types of tactoids labeled A and B, respectively, similar to A and B tactoids of the unheated sample. Heating the sample from room temperature to 150  $^{\circ}\text{C}$  changes the relative peak component area of A from 42 to 35% and that of B from 58 to 65%. This change is associated with thermal water loss and it is concluded that water content in A is higher than in B, suggesting that the tilting of the  $\text{C}_{16}\text{H}_{33}$  chain depends on the water content in the interlayer.

Carbon loss between 150 and 250  $^{\circ}\text{C}$  is 0.7%. This loss is due to air-oxidation of some HDTMA and formation of volatile  $\text{H}_2\text{O}$  and  $\text{CO}_2$ , together with non-volatile intercalated charcoal [17]. At 250  $^{\circ}\text{C}$  only part of the adsorbed organic matter forms LTSC, whereas a greater part persists as HDTMA. Curve fitted diffractogram of the heated sample shows three peak components with maxima at 1.47, 1.41, and 1.37 nm and relative peak component areas 26, 26, and 48%, indicating the presence of three different types of tactoids labeled A, B and C, respectively. Tactoids A and B contain HDTMA and are similar to A and B of 150  $^{\circ}\text{C}$ , whereas C intercalates LTSC.

Thermo-IR-spectroscopy analysis shows that at 360  $^{\circ}\text{C}$  the organic matter is present in the form of charcoal. Carbon loss between 250 and 360  $^{\circ}\text{C}$  is 2.8% due to the completion of HDTMA and the beginning of LTSC oxidation [17]. The fitted diffractogram of OC-41 heated at 360  $^{\circ}\text{C}$  shows three peak components A, B and C with maxima at 1.39, 1.28 and 1.15 nm and relative peak component areas 15, 72 and 13%, respectively. According to the basal spacings tactoids A of 360  $^{\circ}\text{C}$  are similar to C of 250  $^{\circ}\text{C}$ . Namely, the 1.39 nm spacing allows the intercalation of LTSC, making only 15% of the stack. van der Waals diameter of carbon is  $\approx 0.34$  nm suggesting that B with spacing of 1.28 nm intercalates HTSC- $\alpha$ . Spacing of C is too small to intercalate carbon monolayers. It is suggested that C tactoids intercalate HTSC- $\beta$  with carbon atoms imbedded into the ditrigonal holes of the clay-O-planes. Tactoids B have the highest relative component area containing most charcoal of the sample.

There is no carbon loss between 360 and 420  $^{\circ}\text{C}$ . Thermo-IR-analysis shows that the sample heated at 420  $^{\circ}\text{C}$  does not contain HDTMA but contains charcoal

[17]. Three peak components A, B and C appear in the fitted diffractogram of this sample with maxima at 1.39, 1.25 and 1.13 nm and relative peak component areas 3, 72 and 25%, respectively. The low relative area of tactoids A indicates that the heated sample contains very small amounts of LTSC. On the other hand, the relative area of tactoids C (with intercalated HTSC- $\beta$ ) has increased between 360 and 420  $^{\circ}\text{C}$ . It seems that tactoids C intercalate the new HTSC- $\beta$  formed from thermal transformation of LTSC.

Carbon loss between 420 and 550  $^{\circ}\text{C}$  is 4.3%. It results from the oxidation of the charcoal into volatile  $\text{CO}_2$  [17]. The beginning of the dehydroxylation of the clay occurs at this thermal stage. The curve fitted diffractogram of OC-41 heated at 550  $^{\circ}\text{C}$  shows three peak components A, B and C with maxima at 1.12, 1.05 and at 0.99 nm and relative component areas 56, 35 and 9%, respectively. From the spacings it follows that tactoids A are intercalated by monolayers of HTSC- $\beta$ , with carbon atoms embedded in the ditrigonal holes of the clay-O-planes. Collapse of tactoids B is incomplete because some carbon atoms or  $[\text{Ca}(\text{OH})]^+$  cations are trapped in the interlayers, keying into the ditrigonal holes of the clay-O-plane. Tactoids C are fully collapsed indicating that no charcoal persists in the interlayer of these tactoids.

Carbon loss between 550 and 700  $^{\circ}\text{C}$  is 1.4% resulting from the oxidation of HTSC- $\beta$  [17] together with the dehydroxylation of the clay. The fitted diffractogram of OC-41 heated at 700  $^{\circ}\text{C}$  shows two peak components A and B with maxima at 1.03 and 0.96 nm characterizing incomplete and fully collapsed tactoids, respectively. The relative area of the peak component A, with some trapped carbon atoms and/or  $[\text{Ca}(\text{OH})]^+$  cations in the interlayer, is 14%. It is very small compared with that of B (86%) indicating that the oxidation of the charcoal is almost complete.

The effect of the thermal treatment of OC-41 on the homogeneity of the different tactoids is shown by the widths of the peak components (Fig. 4). At 25 and 150  $^{\circ}\text{C}$ , before the formation of charcoal, temperature does not affect the homogeneity. At 250  $^{\circ}\text{C}$  when small amounts of charcoal are present in tactoids C, they become the most homogenous. At 360, 420 and 550  $^{\circ}\text{C}$  tactoids which accommodate HTSC- $\beta$  with carbon atoms imbedded into the ditrigonal holes of the clay-O-plane, have the lowest homogeneity. Collapsed tactoids are the most homogenous, the fully collapsed more than the incomplete collapsed tactoids.

## Second series

Unheated and thermally treated OC-41 are diffracted by X-ray after being suspended in water and overnight air-dried. Results of curve fitting calculations on the diffractograms of

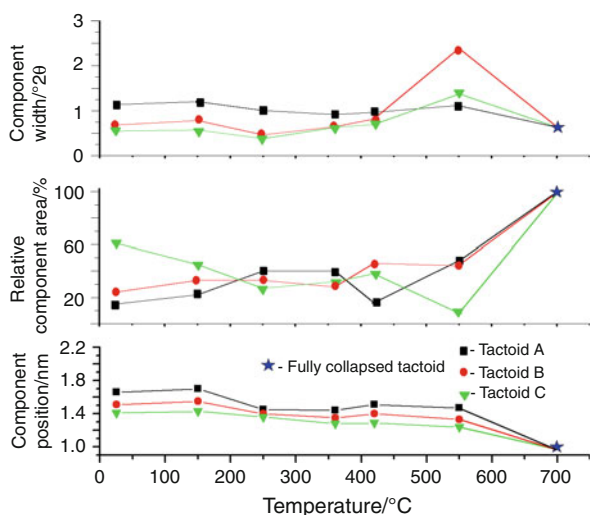


**Fig. 5** Summary of curve fitting calculations on diffractograms of thermo-XRD-analysis of aqueous suspended OC-41 (second series). *Bottom* maxima of peak components (in nm); *middle* relative component areas (in % of the total peak area); *top* component widths at half heights (in  $^{\circ}2\theta$ )

suspended samples are depicted in Fig. 5. Comparing Fig. 4 with Fig. 5 shows that besides OC-41 heated at 700  $^{\circ}\text{C}$ , all samples swell in the suspensions due to water intercalation.

The curve fitting calculations on the diffractogram of the air-dried suspended unheated OC-41 show three peak components, A, B and C at 1.66, 1.51 and 1.41 nm, respectively. Tactoids similar to B and C (with maxima at 1.53 and 1.41 nm) are found in the sample before suspending, but they are labeled A and B. In diffractogram of the non-suspended freeze-dried sample relative areas of components A and B are 42 and 58% and in the diffractogram of the suspended sample relative areas of A, B and C are 15, 24 and 61%, respectively. By comparing these two series it appears that mainly tactoids A of the non-suspended sample swell to 1.66 nm. Basal spacings in the three tactoids allow the presence of intercalated lateral monolayers of HDTMA. In C the long  $\text{C}_{16}\text{H}_{33}$  chain is lying parallel to the clay-O-plane but in A and B this chain is tilted relative to the clay plane.

Air-dried suspended OC-41, heated at 150  $^{\circ}\text{C}$ , before being suspended in water (preheated) results in three types of tactoids A, B and C with basal spacings 1.70, 1.53 and 1.41 nm, respectively. These spacings are slightly larger than those of tactoids of the suspended unheated sample. Comparing Fig. 4 with Fig. 5 shows that tactoids A and B of the non-suspended sample, swell in aqueous suspensions.

Suspending OC-41 preheated at 250  $^{\circ}\text{C}$ , results in three tactoids similar to the tactoids of the non-suspended sample. However, the relative intensities of the peak components differ. Tactoids C with spacing 1.37 nm, which intercalate LTSC, have the highest relative component area

(48%) before suspending, and it becomes the lowest after suspending (27%). Tactoids A with a spacing of 1.47 nm accommodating the non-oxidized HDTMA, have the lowest relative peak component area before suspending (26%) and after suspending it becomes the highest (40%) suggesting that the swelling of tactoids C of the non-suspended OC-41 results in the formation of tactoids intercalated by some kind of hydrated (or hydrolyzed) LTSC with a spacing similar to that of tactoids A of HDTMA-MONT. This requires further study.

Suspending OC-41 preheated at 360  $^{\circ}\text{C}$ , which does not contain HDTMA but contains intercalated charcoal, results in the swelling of the tactoids. Spacings of tactoids A, B, and C in the non-suspended sample are 1.39 (LTSC), 1.28 (HTSC- $\alpha$ ), and 1.13 nm (HTSC- $\beta$ ) with relative peak component areas 15, 72, and 13%. After suspending they become 1.44, 1.35, and 1.28 nm with relative areas 40, 28, and 32%, respectively. The tactoid intercalating HTSC- $\beta$  has been completely rehydrated and does not appear after suspending, suggesting that as a result of the swelling, keying of carbon atoms into the ditrigonal holes of the clay-O-plane does not occur.

Suspending OC-41 preheated at 420  $^{\circ}\text{C}$  results in swelling of the tactoids. Spacings of tactoids A, B, and C before suspending are 1.39, 1.25, and 1.10 nm with relative peak component areas 3, 72, and 25%, and after suspending they become 1.51, 1.40, and 1.29 nm with relative areas 16, 46, and 38%, respectively. The effect of rehydration on the charcoals is similar to its effect on OC-41 preheated at 360  $^{\circ}\text{C}$ .

Suspending OC-41 preheated at 550  $^{\circ}\text{C}$  results in swelling of the tactoids. Spacings of tactoids A, B, and C before suspending are 1.12, 1.05, and 0.99 nm with relative areas 56, 35, and 9%, and after suspending they are 1.47, 1.33, and 1.24 nm with areas 48, 44, and 8%, respectively. Collapsed tactoids disappear after suspending.

Suspending OC-41 preheated at 700  $^{\circ}\text{C}$  does not result in swelling. Only one collapsed tactoid occurs with a basal spacing of 0.97 nm. The incomplete collapsed tactoids which are present before suspending the sample, do not appear in the suspended sample, probably due to the washing out of  $[\text{CaOH}]^+$  cations.

Figure 5 shows that preheating below 550  $^{\circ}\text{C}$  has minor effects on the width of the peak components of the suspended tactoids. The homogeneity of tactoids increases in the order  $\text{C} < \text{B} < \text{A}$ . A different order of homogeneity is obtained for OC-41 preheated at 550  $^{\circ}\text{C}$  with tactoid B being the less homogeneous.

### Third series

Slides of the suspended freeze-dried unheated and preheated OC-41 samples were left 40 days in a desiccator

over silica. Results of curve fitting calculations made on X-ray diffractograms of these oriented samples are depicted in Fig. 6. By comparing Figs. 4 and 5 with Fig. 6, one can see that during desiccation the suspended samples lose only part of the readsorbed water.

Desiccating the suspended unheated OC-41, results in three tactoids with spacings 1.65, 1.48, and 1.41 nm with relative peak component areas 16, 33, and 51% which are similar to those obtained before desiccation. It indicates that the presence of HDTMA in the interlayer, prevents desorption of readsorbed water and contraction.

Desiccating under silica the suspended OC-41 preheated at 150 °C, results in spacing decrease from 1.70, 1.55, and 1.43 nm to 1.54, 1.44, and 1.38 nm with relative peak component areas 23, 26, and 51%, suggesting the desorption of some water.

Desiccating the suspended OC-41 preheated at 250 °C, results in three tactoids with spacings 1.48, 1.40, and 1.36 nm and relative peak component areas 31, 57, and 12% which are similar to those obtained before desiccation. It indicates that the presence of LTSC in the interlayer prevents desorption of readsorbed water.

Desiccating the suspended OC-41 preheated at 360 °C results in three tactoids with spacings of 1.48, 1.37, and 1.28 nm and relative peak component areas of 9, 25, and 66%. The relative area of component C with the smallest spacing is the highest and that of A with the largest spacing is the smallest suggesting escape of some water.

Desiccating the suspended OC-41 preheated at 420 °C results in the appearance of three tactoids with spacings 1.35, 1.27, and 1.23 nm and relative peak component areas of 46, 42, and 12%, respectively. These spacings are

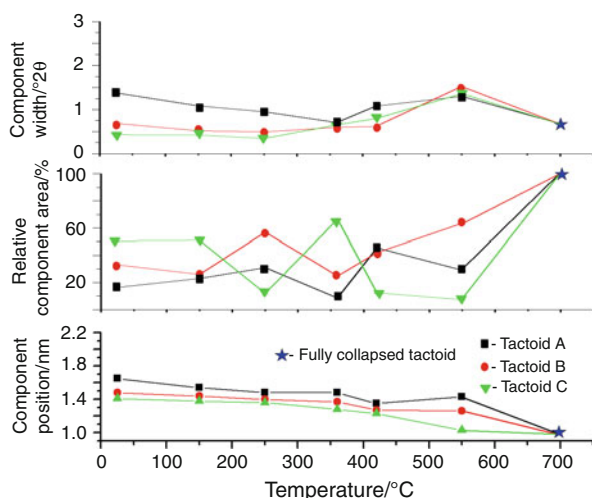


**Fig. 6** Summary of curve fitting calculations on diffractograms of thermo-XRD-analysis of desiccated OC-41 (third series). *Bottom* maxima of peak components (in nm); *middle* relative component areas (in % of the total peak area); *top* component widths at half heights (in  $^{\circ}2\theta$ )

smaller than those recorded before the desiccation due to the escape of some water.

Desiccating the suspended OC-41 preheated at 550 °C results in three tactoids with spacings 1.43, 1.26, and 1.03 nm and relative areas 29, 64, and 7%, respectively. The latter spacing indicates the presence of an incomplete collapsed tactoid. These spacings are higher than those recorded before suspending but are smaller than those recorded before the desiccation, suggesting the escape of part of the adsorbed water.

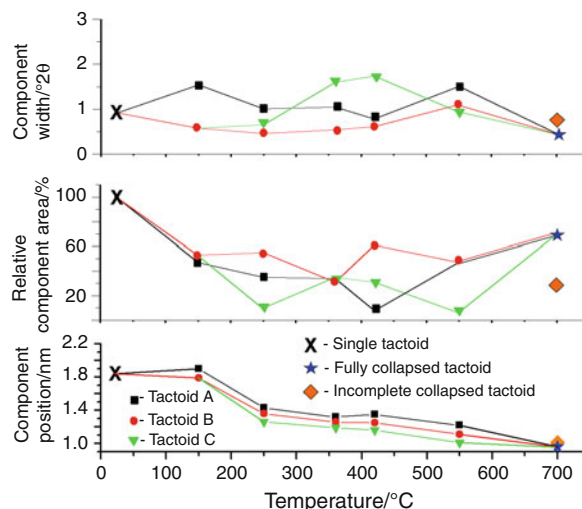
As mentioned above OC-41 preheated at 700 °C does not rehydrate in aqueous suspension and consequently desiccation has no effect on its basal spacing.

Figure 6 shows that the widths of the different components of the silica desiccated samples preheated below 550 °C are only slightly affected by the preheating of the clay. From the width of components of samples preheated below 360 °C it appears that the homogeneity increases from tactoids C to B and further to A. After preheating at 360 °C, with the appearing of HTSC, the homogeneity of B becomes the highest. At 550 °C the homogeneity of the three tactoids decreases.

## OC-90

### First series

Results of curve fitting calculations on the diffractograms recorded during thermo-XRD-analysis of powdered freeze-dried OC-90 are depicted in Fig. 7. Calculations on the



**Fig. 7** Summary of curve fitting calculations on diffractograms of thermo-XRD-analysis of freeze-dried OC-90 (first series). *Bottom* maxima of peak components (in nm); *middle* relative component areas (in % of the total peak area); *top* component widths at half heights (in  $^{\circ}2\theta$ )



diffractogram of unheated OC-90 show a single peak component with a maximum at 1.84 nm, suggesting the existence of one type of tactoids. This spacing allows the intercalation of lateral bilayers HDTMA with the long  $C_{16}H_{33}$  chains being parallel to the clay layers, probably with some water clusters trapped with  $Na^+$  and  $Ca^{2+}$  between the organic cations. The width at half height of this peak ( $0.92^\circ 2\theta$ ) is much smaller than that in the diffractogram of Na-MONT ( $2.83^\circ 2\theta$ ), broader than that of tactoid B of OC-41 ( $0.47^\circ 2\theta$ ) but very similar to that of tactoid A of OC-41 ( $0.99^\circ 2\theta$ ), indicating that the tactoids in the powdered organoclays are more homogeneous than those of the powdered Na-MONT.

In part 1 of this study, at 150 °C carbon analysis did not show any carbon loss and thermo-IR spectroscopy analysis of OC-90 showed the persistence of HDTMA. It indicates that no organic matter is evolved at 150 °C and mass loss resulted from water evolution [17]. By comparing this loss (3.2%) with those of Na-MONT and OC-41 at the same temperature range (8.6 and 4.4%, respectively [17]), it appears that water content decreases with the loading of the organic cation [25, 26].

The fitted diffractogram of OC-90 heated at 150 °C shows two peak components at 1.90 and 1.79 nm with relative peak component areas 47% and 53%, suggesting the presence of two types of tactoids labeled A and B, respectively. Interlayer spaces in both tactoids allow the presence of HDTMA bilayers lying parallel to the clay layers. The decrease in spacing of tactoid B from 1.84 nm (unheated) to 1.79 nm (heated at 150 °C) is associated with the escape of interlayer water accompanied by a decrease in the angle in which the  $C_{16}H_{33}$  chains are tilted relative the clay-O-planes. On the other hand, the increase in spacing of tactoid A from 1.84 to 1.90 nm (after heating) suggests an increase of the angle in which the  $C_{16}H_{33}$  chains are tilted relative to the planes. Widths of components A and B are 1.54 and  $0.57^\circ 2\theta$ , respectively, suggesting that the homogeneity of tactoids A, with the tilted chain, is smaller than that of B. Homogeneity of tactoids B of OC-90 is similar to that of tactoids B of OC-41, but that of tactoids A of the former is smaller than that of the latter. However, both are much more homogeneous than Na-MONT heated at 150 °C.

Carbon loss between 150 and 250 °C is 7.2%. This loss is due to air-oxidation of significant amounts of HDTMA and formation of volatile  $H_2O$  and  $CO_2$ , together with non-volatile intercalated charcoal [17]. This loss of OC-90 is high compared with that of OC-41 (0.7%). This is in agreement with our previous conclusion based on DTG, carbon analysis and thermo-IR-spectroscopy that the oxidation of HDTMA in OC-90 at this stage is significant, but in OC-41 it requires higher temperatures.

Fitted diffractogram of OC-90 heated at 250 °C shows three peak components A, B and C with maxima at 1.43,

1.36, and 1.26 nm and relative peak component areas 35, 55, and 10%. From these spacings it appears that tactoids A intercalate monolayers of non-oxidized HDTMA, tactoids B and C intercalate LTSC and HTSC- $\alpha$ , respectively, the latter in small amounts. Widths at half height are 1.01, 0.46, and  $0.65^\circ 2\theta$ , respectively, indicating that tactoids A with intercalated non-oxidized HDTMA are the less homogeneous whereas those with charcoal layers are more homogeneous.

Thermo-IR-spectroscopy analysis shows that at 360 °C the organic matter occurs as charcoal. Carbon loss between 250 and 360 °C is 1.8% due to completion of HDTMA oxidation and beginning of LTSC oxidation [17]. Three peak components A, B, and C appear in the curve fitted diffractogram of OC-90 heated at 360 °C with maxima at 1.32, 1.26, and 1.19 nm, relative peak component areas 34, 31, and 35% and widths at half heights 1.05, 0.54, and  $1.60^\circ 2\theta$ , respectively. From spacings it appears that tactoids A intercalate LTSC whereas B and C intercalate HTSC- $\alpha$  and HTSC- $\beta$ , respectively. Peak component C has the highest width indicating that tactoids C are the less homogeneous in the stuck and tactoids B are the most homogeneous.

Carbon analysis showed no carbon loss between 360 and 420 °C [17]. The fitted diffractogram of OC-90 heated at 420 °C shows three peak components A, B, and C with maxima at 1.35, 1.25, and 1.16 nm, relative peak component areas 8, 61, and 31% and widths at half heights of 0.78, 0.61, and  $1.74^\circ 2\theta$ , respectively. The diffractogram of this sample is almost similar to that of the sample heated at 360 °C. It is only that the relative peak component area of A decreases and that of B increases with the rise in temperature, indicating that the LTSC which intercalates tactoids A at 360 °C is thermally transformed to HTSC- $\alpha$  at 420 °C. Tactoids intercalating HTSC- $\beta$  have the lowest homogeneity whereas those intercalating HTSC- $\alpha$  are the most homogeneous.

Carbon loss between 420 and 550 °C is 6.0% [17]. The oxidation of HTSC starts at this thermal stage together with the dehydroxylation of the clay. The fitted diffractogram of OC-90 heated at 550 °C shows three peak components A, B and C with maxima at 1.22, 1.12, and 1.01 nm and relative areas of 47, 47, and 6%. Tactoids C are incomplete collapsed, indicating that they do not intercalate charcoal. HTSC- $\alpha$  and HTSC- $\beta$  intercalate tactoids A and B, respectively. Widths at half heights are 1.51, 1.11, and  $0.93^\circ 2\theta$ , respectively, suggesting that A is the most inhomogeneous and C, with no charcoal is the most homogeneous, but its concentration is very small.

Carbon loss between 550 and 700 °C is 2.3% due to the oxidation of HTSC. The curve-fitted diffractogram of OC-90 heated at 700 °C shows two peak components at 1.01 (30%) and 0.96 (70%) nm. These spacings characterize

incomplete and fully collapsed tactoids, respectively. As mentioned above, incomplete collapse may result from the presence of some trapped  $[\text{Ca}(\text{OH})]^+$  cations and/or carbon atoms. Widths at half height are 0.75 and 0.46  $^{\circ}2\theta$ , respectively, indicating that the homogeneity of the fully collapsed tactoids is higher than that of the incomplete collapsed tactoids.

### Second series

Unheated and thermally treated OC-90 samples are diffracted by X-ray after being suspended in water and overnight air-dried. Results of curve fitting calculations on the diffractograms of these samples are depicted in Fig. 8. Comparing Fig. 7 with Fig. 8 reveals that besides OC-90 heated at 700  $^{\circ}\text{C}$ , all samples expand in the aqueous suspensions due to water intercalation. Beside the sample heated at 700  $^{\circ}\text{C}$ , the curve fitting calculations of the rehydrated freeze-dried and thermal-treated OC-90 diffractograms show three peak components, A, B and C, suggesting the presence of three different types of tactoids.

Samples with no charcoal, namely, the unheated and that heated at 150  $^{\circ}\text{C}$ , spacings of A, B and C are 2.13, 1.98 and 1.82 nm. Comparing these spacings with those of the non-suspended unheated OC-90 suggests that tactoids A and B are the swelling products of tactoids with basal spacings 1.84 or 1.79 nm. A spacing of 2.13 nm allows the presence of a water monolayer between two parallel layers of HDTMA [6]. A spacing of 1.98 nm may occur from regular interstratification of 2.13 and 1.82 nm interlayers. Relative component areas in diffractograms of suspended

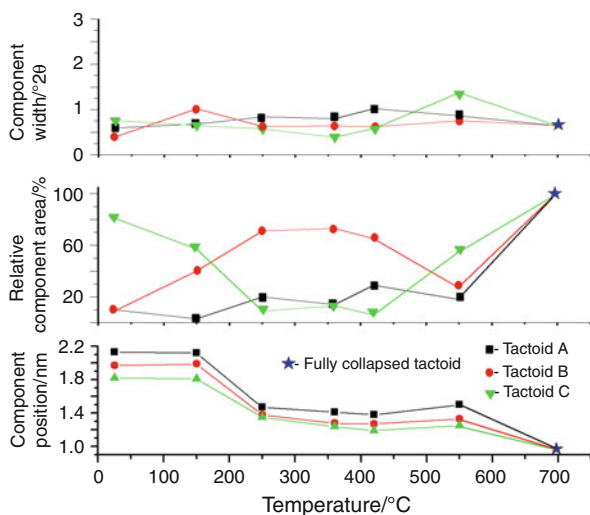


**Fig. 8** Summary of curve fitting calculations on diffractograms of thermo-XRD-analysis of aqueous suspended OC-90 (second series). *Bottom* maxima of peak components (in nm); *middle* relative component areas (in % of the total peak area); *top* component widths at half heights (in  $^{\circ}2\theta$ )

unheated or preheated at 150  $^{\circ}\text{C}$ , are 10, 9, and 81%, or 3, 40, and 57% of total peak area, respectively, indicating that heating at 150  $^{\circ}\text{C}$  improves the water adsorption abilities.

OC-90 heated at 250  $^{\circ}\text{C}$  contains mainly charcoal with some non-oxidized HDTMA [17]. A fitted diffractogram of the suspended sample shows three peak components with maxima at 1.47 (HDTMA), 1.38 (LTSC) and 1.35 nm (HTSC- $\alpha$ ) and relative areas 20, 71, and 9%, respectively. If these spacings and relative areas are compared with those of the non-suspended sample (1.43, 1.36 and 1.26 nm with areas 35, 55, and 10%) it is obvious that the tactoids adsorb small amounts of water into the interlayers. If these spacings are compared with those of the suspended 150  $^{\circ}\text{C}$  treated OC-90, it appears that swelling ability decreases with the rise in temperature.

Suspending OC-90 preheated at 360 or 420  $^{\circ}\text{C}$ , results in three tactoids with spacings 1.41, 1.28, and 1.24 nm, in the former and 1.38, 1.27, and 1.19 nm, in the latter. Relative peak component areas are 14, 73, and 13% in the former and 29, 65, and 6% in the latter. These spacings are slightly higher than those of the non-suspended 360 and 420  $^{\circ}\text{C}$  treated OC-90 (Fig. 4) indicating that the three charcoal-clay tactoids have only small swelling abilities. Comparing these spacings with those of the suspended OC-90 preheated at 250  $^{\circ}\text{C}$ , suggests that the swelling ability of the charcoal-clay slightly decreases with the rise in temperature of the thermal treatment.

Suspending OC-90 preheated at 550  $^{\circ}\text{C}$ , results in three tactoids with spacings 1.50, 1.33, and 1.26 nm and relative peak component areas 18, 27, and 55%. If these spacings are compared with those of the non-suspended heated sample and with those of suspended sample preheated at 420  $^{\circ}\text{C}$ , it is obvious that the hydration and swelling abilities of this clay are better than those of the sample heated at 420  $^{\circ}\text{C}$ . This may be due to the thermal oxidation of some of the intercalated charcoal.

The sample heated at 700  $^{\circ}\text{C}$  is collapsed and does not rehydrate by suspending. Only fully collapsed tactoids occur with a basal spacing 0.98 nm. The incomplete collapsed tactoids which are present in this sample before being suspended, are not detected in the suspended sample, probably due to the washing out of  $[\text{CaOH}]^+$  cations.

The effect of temperature of pretreatment on the homogeneity of the different tactoids is studied from the widths of the respective components. Figure 8 shows that in suspended samples, unheated and preheated between 250 and 420  $^{\circ}\text{C}$  tactoids of type A with the largest spacings, are less homogeneous than those of type B.

### Third series

Slides of suspended unheated and preheated OC-90 samples were left 40 days in a desiccator over silica. Results of

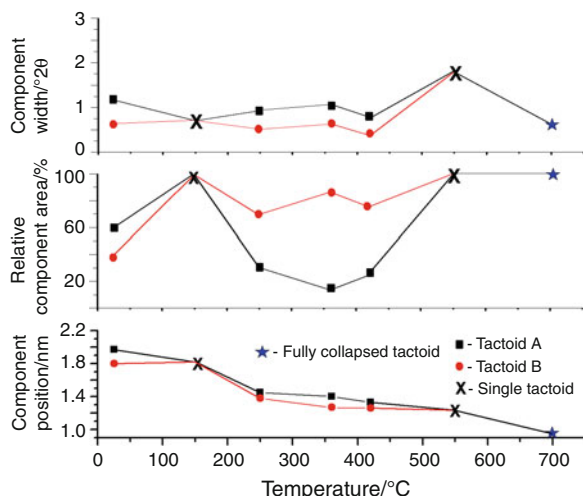


**Fig. 9** Summary of curve fitting calculations on diffractograms of thermo-XRD-analysis of desiccated OC-90, (Third series). *Bottom* maxima of peak components (in nm); *middle* relative component areas (in % of the total peak area); *top* component widths at half heights (in  $^{\circ}2\theta$ )

curve fitting calculations made on the X-ray diffractograms of these oriented samples are depicted in Fig. 9. By comparing between Figs. 7 and 8 with Fig. 9 it can be seen that the rehydrated samples lose only part of the readsorbed water during desiccation.

As mentioned above, suspended unheated OC-90 contains three tactoid types A, B, and C with spacings 2.13, 1.97, and 1.82 nm and relative peak component areas of 10, 9, and 81%, respectively. After desiccating under silica it contains two tactoid types with spacings 1.97 and 1.80 nm and relative peak component areas of 60 and 40% of the total peak area, suggesting that partial water desorption occurs. The presence of HDTMA in the interlayer prevents a complete dehydration of the clay.

Desiccating under silica the suspended OC-90 preheated at 150  $^{\circ}\text{C}$  results in a single type of tactoids with spacing of 1.80 nm, suggesting desorption of some water.

Desiccating the suspended OC-90 preheated at 250  $^{\circ}\text{C}$  results in two tactoid types with spacings 1.45 and 1.38 nm and relative peak component areas 30 and 70%. The relative component areas and the non-appearing of the 1.35 nm tactoid of the non-suspended sample suggest that this sample does not dehydrate under silica.

Desiccating the suspended OC-90 preheated at 360  $^{\circ}\text{C}$  results in two types of tactoids with spacings 1.40 and 1.27 nm and relative component areas of 14 and 86%. They are similar to those obtained before desiccation. The relative component areas and the non-appearing of the 1.24 nm of the non-suspended sample suggest that this sample does not dehydrate under silica.

Desiccating the suspended OC-90 preheated at 420  $^{\circ}\text{C}$  results in two types of tactoids with spacings 1.33 and 1.26 nm and relative areas 25 and 75% similar to those obtained before desiccation. These data and the non-appearing of the 1.19 nm tactoid, detected before desiccating, suggest that this sample does not dehydrate.

Desiccating OC-90 preheated at 550  $^{\circ}\text{C}$  results in a single tactoid with spacing of 1.24 nm. This spacing is smaller than those of the tactoids of the suspended sample (1.50, 1.33, and 1.25 nm) suggesting that this sample dehydrates during desiccation.

As mentioned above OC-90 preheated at 700  $^{\circ}\text{C}$  does not rehydrate in aqueous suspension and consequently desiccation has no effect on its basal spacing.

According to Fig. 9 there is almost no effect of temperature of the preheating on the widths of the different peak components of the silica desiccated tactoids, and besides the sample heated at 550  $^{\circ}\text{C}$ , the desiccated tactoids are relatively homogeneous. In samples which

**Table 1** X-ray diffraction data for Na-montmorillonite (Wyoming bentonite) and of OC-41 and OC-90 heated to 900  $^{\circ}\text{C}$

Mineral (after [27, 28])	Na-montmorillonite		OC-41		OC-90	
	Nm	Relative intensity	Nm	Relative intensity	Nm	Relative intensity
Spinel [27]; Quartz [28]	0.427	23.0	0.427	25.0	0.426	38.0
Cristobalite [27, 28]	0.408	18.5	0.408	20.0	0.405	21.1
	0.349	25.7				
	0.343	17.9	0.343	19.1		
Quartz [27, 28]	0.336	100.0	0.335	100.0	0.334	100.0
(003) Anhydrous [27]	0.320	16.2	0.320	10.7	0.319	13.7
Spinel [27]	0.286	10.7	0.283	5.6	0.283	1.7
	0.269	4.3				
Spinel [27]	0.252	11.1				
Spinel [27]; Quartz [28]	0.244	16.2	0.242	11.1	0.243	12.0
	0.233	4.6				
Quartz [28]	0.229	6.2	0.229	3.5	0.228	3.7

contain two tactoids the one with the higher spacing (tactoid A) is the less homogeneous.

### Samples thermally treated at 900 °C

Mass loss of Na-MONT, OC-41, and OC-90 in the temperature range 25–900 °C are 15.8, 23.2, and 32.6%, respectively, calculated from TG curves [17]. At 900 °C MONT dehydroxylates and most of the solid phase become amorphous and do not diffract X-ray. A very small fraction of this phase undergoes thermal recrystallization. Table 1 summarizes the spacings of the recrystallization products and their intensities relative to the 101 reflection of quartz, present as a trace impurity in Na-MONT, OC-41, and OC-90. From the table it appears that after heating at 900 °C there are no significant differences between the three clays. Our results for Na-MONT are in good agreement with previous studies [27]. Spacings of quartz and cristobalite are supplemented by data from JCPDS [28].

### Conclusions

Very little is known on the structure and properties of charcoal-clay tactoids. This study demonstrates that thermo-XRD-analysis combined with curve fitting calculations on diffractograms recorded after heating the organoclay at different temperatures is useful in the study of the different tactoids of organo-MONT and of charcoal-MONT obtained during thermal treatments. This information is required in order to be able to apply these nanocomposites in modern technologies.

Different numbers of cation exchange sites are occupied by HDTMA in OC-41 and OC-90. This should affect the intergallery confinement of the cation, and consequently, many of the properties of the former should differ from those of the latter [29, 30]. Indeed, OC-41 intercalates monolayers of HDTMA whereas OC-90 intercalates bilayers. As well, the thermal behavior differs. When OC-41 is air-heated, oxidation of HDTMA and formation of charcoal-MONT tactoids occurs to a small extent at 250 °C. On the other hand, when OC-90 is heated at 250 °C, great part of the HDTMA is oxidized and charcoal-MONT tactoids are formed. With the rise in temperature the organic matter is gradually oxidized in both organoclays. At 700 °C most MONT is dehydroxylated forming an amorphous phase and the remaining clay is collapsed. At 900 °C the recrystallization of the amorphous phase begins. At this stage there are no significant differences between the thermal products obtained from Na-MONT, OC-41, or OC-90.

During the thermo-XRD-analysis of both organoclays, combined with curve fitting calculations on the diffractograms, the following spacings are used in the identification of the

different tactoids. HDTMA-MONT tactoids are identified in the fitted diffractograms from maxima at  $\geq 1.41$  nm. They occur between 25 and 250 °C. Incomplete collapsed tactoids are identified by a maximum at 1.01–1.05 nm. They occur between 550 and 700 °C. Fully collapsed tactoids are identified by a maximum at 0.96–0.98 nm. They occur at 700 °C. Three types of charcoal-MONT complexes are identified in this study: (1) LTSC-MONT tactoids identified by a maximum at 1.32–1.39 nm, occur between 250 and 420 °C in both organoclays; (2) HTSC- $\alpha$ -MONT tactoids identified by a maximum at 1.22–1.28 nm, occur between 360 or 250 and 500 or 550 °C in OC-41 or OC-90, respectively; (3) HTSC- $\beta$ -MONT showing a maximum at 1.12–1.18 nm, occur between 360 and 550 °C in both organoclays. HTSC- $\beta$ -MONT differs from HTSC- $\alpha$ -MONT by having carbon atoms keying into the ditrigonal holes of the clay-O-planes.

OC-41 and OC-90 unheated or preheated up to 550 °C adsorb water from aqueous suspensions and swell, but samples preheated at 700 °C do not swell. Desiccation under silica leads to some water desorption of OC-41 tactoids. In the case of OC-90, only samples which are preheated at 150 or 550 °C lose some water. It seems that the presence of charcoal in the interlayer space slows down desorption of water from the rehydrated clays. Samples preheated at 550 °C have lost most of the charcoal and, therefore, lose water upon desiccation.

Thermo-XRD-analysis of freeze-dried Na-MONT reveals that some collapsed tactoids are present after heating the clay at 250 °C. But the complete transformation of Na-MONT into collapsed clay occurs at 360 °C. Besides collapsed Na-MONT obtained at 700 °C, all collapsed tactoids obtained at lower temperatures swell when they are suspended in water.

Tactoids of organoclays are more homogeneous than those of Na-MONT. The dependency of homogeneity of the different tactoids, obtained during the thermal treatments, on the intercalated charcoals requires further study.

**Acknowledgements** Help from Nadezhda Bukhanovsky (The Volcani Center, Agricultural Research Organization, Israel) in preparing the thermally treated organoclay samples is appreciated. This research was supported by a grant from the Israeli Science Foundation (No. 919/08) and by a grant from the Ministry of Science, Culture and Sport, Israel and the Ministry of Research (Infrastructure 3-4136).

### References

1. Theng BKG. The chemistry of clay-organic reactions. London: Adam Hilger; 1974.
2. Lagaly G. Clay organic reactions. *Philos Trans R Soc Lond.* 1984;A311:89–167.
3. Giese RF, van Oss CJ. Organophilicity and hydrophobicity of organoclays. In: Yariv S, Cross H, editors. *Organo-clay complexes and interactions*. New York: Marcel Dekker; 2002. p. 175–91.

4. Murray HH. Clays for our future. In: Kdama H, Mermut AR, Kennet Torrance J, editors. Proc 11th intern clay conf Ottawa 1997. Boulder: The Clay Mineral Society; 1999. p. 3–11.
5. Borisover M, Bukhanovsky N, Lapides I, Yariv S. Thermal treatment of organoclays: effect on the aqueous sorption of nitrobenzene on *n*-hexadecyltrimethyl ammonium montmorillonite. *Appl Surf Sci*. 2010;256:5539–44.
6. Burstein F, Borisover M, Lapides S, Yariv S. Secondary adsorption on nitrobenzene and *m*-nitrophenol by hexadecyltrimethylammonium-montmorillonite: Thermo-XRD-analysis. *J Therm Anal Calorim*. 2008;92:35–42.
7. Borisover M, Gerstl Z, Burshtein F, Yariv S, Mingelgrin U. Organic sorbate-organoclay interactions in aqueous and hydrophobic environments: sorbate-water competition. *Environ Sci Technol*. 2008;42:7201–6.
8. Ovadyahu D, Lapides I, Yariv S. Thermal analysis of tributylammonium montmorillonite and Laponite. *J Therm Anal Calorim*. 2007;87:125–34.
9. Langier-Kuzniarowa A. Thermal analysis of organo-clay complexes. In: Yariv S, Cross H, editors. *Organo-clay complexes and interactions*. New York: Marcel Dekker; 2002. p. 273–344.
10. Yariv S. Differential thermal analysis (DTA) in the study of thermal reactions of organo-clay complexes. In: Ikan R, editor. *Natural and laboratory simulated thermal geochemical processes*. Dordrecht: Kluwer Academic Publishers; 2003. p. 253–96.
11. Yariv S. The role of charcoal on DTA curves of organoclay complexes: an overview. *Appl Clay Sci*. 2004;24:225–36.
12. Yermiyahu Z, Landau A, Zaban A, Lapides I, Yariv S. Mono-ionic montmorillonites treated with Congo-red: differential thermal analysis. *J Therm Anal Calorim*. 2003;72:431–41.
13. Yermiyahu Z, Lapides I, Yariv S. Thermo-XRD-analysis of montmorillonite treated with protonated Congo-red: curve fitting. *Appl Clay Sci*. 2005;30:33–41.
14. Yermiyahu Z, Kogan A, Lapides I, Pelly I, Yariv S. Thermal study of naphthylammonium- and naphthylazonaphthylammonium-montmorillonite. XRD and DTA. *J Therm Anal Calorim*. 2008;91:125–35.
15. Green-Kelly R. The montmorillonite minerals (smectites). In: Mackenzie RC, editor. *The differential thermal investigation of clays*. London: Mineralogical Society (Clay Minerals Group); 1957. p. 140–64.
16. Yariv S, Borisover M, Lapides I. Few introducing comments on the thermal analysis of organoclays. *J Therm Anal Calorimim*. 2011. doi:10.1007/s10973-010-1221-y.
17. Lapides I, Borisover M, Yariv S. Thermal-analysis of hexadecyltrimethylammonium-montmorillonites. Part 1: thermogravimetry, carbon and hydrogen analysis and thermo-IR-spectroscopy-analysis. *J Therm Anal Calorimim*. 2011. doi:10.1007/s10973-011-1304-4.
18. He H, Ding Z, Zhu J, Yuan P, Xi Y, Yang D, Frost RL. Thermal characterization of surfactant-modified montmorillonite. *Clays Clay Min*. 2005;53:287–93.
19. Yariv S, Lapides I. The use of thermo-XRD-analysis in the study of organo-smectite complexes. *J Therm Anal Calorim*. 2005;80:11–26.
20. Yariv S. Wettability of clay minerals. In: Schrader ME, Loeb G, editors. *Modern approach to wettability*. New York: Plenum Press; 1992. p. 279–326.
21. Cases J, Berend I, Besson G, Francois M, Uriot JP, Thomas F, Poirier JE. Mechanism of adsorption and desorption of water vapor by homoionic montmorillonite: I the sodium exchanged form. *Langmuir*. 1992;11:2734–41.
22. MacEwan DMC, Wilson MJ. Interlayer and intercalation complexes of clay minerals. In: Brindley GW, Brown G, editors. *Crystal structures of clay minerals and their X-ray identification*. Monograph. Vol 5. London: Mineralogical Society; 1980. p. 197–248.
23. Newman ACD, Brown G. The chemical constitutions of clays. In: Newman ACD, editor. *Chemical composition of clays and clay*. Minerals mineralogical society monograph no 6. London: Longman Scientific and Technical; 1987. p. 1–128.
24. Marshall CE. *The colloid chemistry of silicate minerals*. New York.: Academic Press, Inc.; 1949.
25. Jordan JW. Organophilic bentonites I. Swelling in organic liquids. *J Phys Colloid Chem*. 1949;53:294–306.
26. Jordan JW. Alteration of the properties of bentonite by reaction with amines. *Mineralog Mag*. 1949;28:598–605.
27. Earley JW, Milne IH, McVeagh WJ. Dehydration of montmorillonite. *Am Miner*. 1953;38:770–83.
28. JCPDS. International center for diffraction data. Quartz, PDF # 89-1961; cristobalite, PDF # 82-0512; 2001.
29. Vianna MMGR, Dweck J, Quina FH, Carvalho FMS, Nascimento CAO. Toluene and naphthalene sorption by iron oxide/clay composites Part II. Sorption experiments. *J Therm Anal Calorim*. 2010;101:887–92.
30. Ganguly S, Dana K, Ghatak S. Thermogravimetric study of *n*-alkylammonium-intercalated montmorillonites of different cation exchange capacity. *J. Therm. Anal. Cal*. 2010;100:71–8.